

Could stratospheric ozone depletion lead to enhanced aquatic primary production in the polar regions?

Børge Hamre, Jakob J. Stannnes, and Øyvind Frette

Department of Physics and Technology, University of Bergen, Allégaten 55, NO-5007 Bergen, Norway

Svein Rune Erga

Department of Biology, University of Bergen, Jahnebakken 5, NO-5020 Bergen, Norway

Knut Stannnes

Department of Physics and Engineering Physics, Stevens Institute of Technology, Hoboken, New Jersey 07030

Abstract

We study the effects of ozone depletion on primary production in ice-covered and open polar waters using a spectral radiative transfer model combined with a parameterization of the inhibition of marine photosynthesis by ultraviolet radiation. We find that ozone depletion might not have a negative influence on the aquatic algal community at high latitudes but instead could enhance primary production. For an ozone depletion of 50%, we estimate the yearly averaged enhancement to be about 1%.

Even though ozone-destroying chemicals are mostly phased out of production, they will reside in the atmosphere for the next few decades and continue to deplete stratospheric ozone. In addition, global warming could indirectly, through increased formation of stratospheric ice clouds, increase the destruction of ozone (Austin et al. 1992; Staehelin et al. 2001). Various studies have suggested that one effect of ozone depletion on aquatic ecosystems could be a reduction in primary production because of increased ultraviolet B (UVB; $280 < \lambda < 320$ nm) radiation (Häder 1997). Smith et al. (1992) estimated a reduction in primary production of about 6–12% in the marginal ice zone in the Southern Ocean with a stratospheric ozone reduction from 300 to 200 Dobson units (DU). At about the same time, Holm-Hansen et al. (1993) estimated the reduction in daily primary production under a well-developed ozone hole (150 DU) in Antarctica to be <3.8%. Five years later, Neale et al. (1998b) predicted that an ozone depletion from 300 to 150 DU would lead to a reduction in primary production of between 8.5% and 0.7% for clear sky conditions and between 6.2% and 0.8% under cloudy skies.

Our calculations show that these previous estimates of reductions in primary production because of increased levels of ultraviolet radiation might be too large and that

ozone depletion could lead to increased annual primary production in polar regions. Such a reduction is possible, as explained later in this paper, because ozone depletion not only causes increased levels of UVB radiation, but also increased levels of photosynthetically available radiation (PAR; $400 < \lambda < 700$ nm), and because a large fraction of the primary production in polar regions occurs under low solar elevations and in environments that are protected from UVB radiation by snow-covered sea ice. The possibility of enhanced marine production because of increased PAR was discussed by Arrigo (1994). On the basis of model calculations for the early spring at 75°S , he predicted that a 50% reduction of stratospheric ozone would cause a 9% enhancement of the depth-integrated production. However, because the mean solar zenith angle decreases in the late spring and summer, he found reduced production, caused by increased inhibition by UVB radiation, to be dominating. Integrating over the light cycle and from the surface down to the base of the euphotic zone in open water, he found the reduction in primary production because of increased UVB radiation to be <1%. Later, Arrigo et al. (2003) found that the reduction in spring primary production would be <0.25% in Antarctica. In this paper, we address the potential effect of ozone depletion on primary production in both open waters and ice-covered waters for varying solar zenith angles and latitudes.

Acknowledgments

This work was supported by the Norwegian Research Council. K.S. acknowledges support from the National Science Foundation, Office of Polar Programs, via a grant to Stevens Institute of Technology. We also thank the Editor and two reviewers for valuable comments. The action spectra for UVR induced inhibitions in photosynthesis was provided by the National Science Foundation Ultraviolet Monitoring Network, operated by Biospherical Instruments Inc. under a contract from the United States National Science Foundation's Office of Polar Programs via Raytheon Polar Services Company.

Model description

Marine photosynthesis can be parameterized as in Eq. 1 (Cullen et al. 1992; Neale et al. 1998a).

$$P = P_s \left(1 - e^{-E_p/E_s} \right) \frac{1}{1 + E^*} \quad (1)$$

Here, P_s is the maximum photosynthesis in the absence of photo inhibition. The unit of P is the same as the unit of P_s , which is usually mass carbon produced per mass chloro-

phyll *a* [Chl *a*] per time or mass oxygen produced per mass Chl *a* per time. Throughout this paper, photosynthesis and primary production are used as equivalent terms and defined without respiratory losses. E_p in Eq. 1 is the photosynthetically utilizable radiation (PUR), which is the PAR weighted by the absorption spectrum (Morel 1974).

$$E_p = \int_{400}^{700} E_0(\lambda) a^*(\lambda) d\lambda \quad (2)$$

Here, $E_0(\lambda)$ is the scalar irradiance (i.e., the radiance integrated over all 4π directions), and $a^*(\lambda)$ is the normalized algal absorption spectrum (Fig. 1B). In Eq. 1, E_s is the PUR saturation level, which determines the slope of P as E_p approaches zero. Furthermore, the factor $\frac{1}{1+E^*}$ in Eq. 1 describes the inhibition caused by ultraviolet radiation (UVR; $\lambda < 400$ nm), where E^* is the wavelength-integrated scalar irradiance weighted by an action spectrum $\varepsilon(\lambda)$ for UVR-induced inhibition of photosynthesis (Fig. 1A; see also Fig. 4),

$$E^* = \int_{280}^{400} \varepsilon(\lambda) E_0(\lambda) d\lambda \quad (3)$$

The photosynthesis described by these equations depends on the UVR dose rate, implying that a change in the UVR level will cause an instantaneous change in photosynthesis. Consequently, photosynthesis is independent of the light history experienced by each individual algae, which makes the depth-integrated photosynthetic production independent of oceanic mixing rates.

Parameterizations in which production, inhibition, and recovery depend on both current radiation levels and radiation history are commonly referred to as dose dependent (Neale et al. 1998a). Arrigo et al. (2003) found that the use of a dose rate-dependent model instead of a dose-dependent model might cause a small underestimation of the harmful effects of UVR. In their calculations for the spring in the Antarctic region, they found the dose-dependent model to give twice as much loss in primary production during ozone depletion as the dose rate-dependent model. However, it is not well known which of these two models describes nature most accurately. We therefore use the dose rate-dependent model and note that our results would be slightly modified with the use of a dose-dependent model but that the overall conclusions should not be affected.

The solar irradiance $E_0(\lambda)$ that drives and inhibits primary photosynthesis depends on a number of environmental factors, such as the total ozone column amount, the solar zenith angle, and the depth in the ocean, as well as on the presence of clouds, ice, and snow. We determined the scalar irradiance under changing environmental conditions by employing a multistream radiative transfer model for the coupled atmosphere–snow–sea ice–ocean system (Jin and Stamnes 1994; Thomas and Stamnes 1999). The model has been used and tested in a number of applications (see, e.g., Jin et al. 1994; Gjerstad et al. 2003). Assuming total ozone column amounts of 400 DU and 200 DU, we

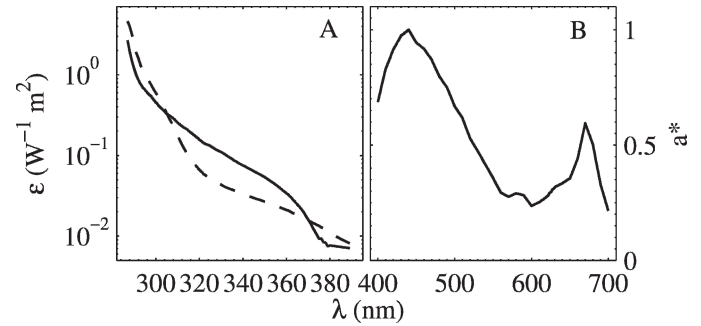


Fig. 1. (A) Action spectrum for UVR-induced inhibition of photosynthesis. The solid line represents an average over phytoplankton from the Southern Ocean (www.biospherical.com/nsf), and the dashed line represents *Phaeodactylum* sp. (Cullen et al. 1992). (B) Action spectrum for PUR-induced photosynthesis (Prieur and Sathyendranath 1981).

computed the scalar irradiance at the bottom of snow-covered sea ice and at various depths of open water. We did not include highly UVR absorbing impurities like soot, dust, and organic matter in the snow and the ice to make sure not to provide extra UVR protection for the ice algae growing in the bottom layer of the ice. Our choice of 400 DU as a “normal” total ozone column amount was based on measured ozone values in the Arctic in the spring (see, e.g., <http://toms.gsfc.nasa.gov/>), making 200 DU a hypothetical 50% reduction. In our calculations, we set the PUR saturation level E_s in Eq. 1 to 5 W m^{-2} , which is an average (after conversion to PUR) of E_s values for ice algae and open-water phytoplankton given by Sakshaug et al. (1990) and Johnsen and Hegseth (1991). Unless otherwise specified, the parameters in Table 1 were used in the computations throughout this paper. See also Hamre et al. (2004) for further details about parameterizations and optical properties of the atmosphere, snow, sea ice, and ocean.

Results and discussion

First, we carry out a simple analysis to determine how photosynthesis responds to a relative change in PAR and UVR levels. Letting $E_p/E_s = E'$ and taking the total differential of Eq. 1, we get Eq. 4.

$$\frac{dP}{P} = \frac{E'}{e^{E'} - 1} \frac{dE'}{E'} - \frac{E^*}{1 + E^*} \frac{dE^*}{E^*} \quad (4)$$

We see that for *large* values of both E' and E^* (i.e., for large values of both PUR and UVR), $E'/(e^{E'} - 1) \rightarrow 0$ and $E^*/(1 + E^*) \rightarrow 1$, so that Eq. 4 reduces to $dP/P = -dE^*/E^*$. Thus, for high radiation levels, a relative increase in E^* (UVR) causes an equally large relative reduction in photosynthesis, whereas a simultaneous relative increase in E' (PUR) has no effect. However, for *small* values of both E' and E^* , $E'/(e^{E'} - 1) \rightarrow 1$ and $E^*/(1 + E^*) \rightarrow 0$. Now a relative increase in E' or PUR causes an equally large relative increase in photosynthesis, whereas a simultaneous increase in UVR has no effect. Normally E' and E^* have values between the two extremes considered above. But

Table 1. Summary of optical properties and physical parameters used in the radiative transfer computations. The atmosphere constituents and the aerosol extinctions were obtained from Andersen et al. (1986) and Shettle and Fenn (1976). Note that snow and ice are only present in Figs. 6, 7, and 9.

Property	Value
Atmosphere	
Subarctic winter	
Aerosol optical depth at 550 nm	0.10
Clouds (if present)	
Liquid water content	0.2 g m ⁻³
Droplet radius	7 μm
Thickness	300 m
Snow (if present)	
Thickness	5 cm
Density	250 kg m ⁻³
Ice (if present)	
Thickness	50 cm
Density	920 kg m ⁻³
Salinity	0.5‰
Temperature	-2°C
Ocean	
Chl <i>a</i> concentration	1.0 mg m ⁻³

for low solar elevations at sufficiently deep levels in the ocean or under snow-covered ice, where both the UV and visible radiation levels are small, an increase in UVR will have a small effect on primary production, whereas a relative increase in PUR will cause a corresponding relative increase in photosynthesis. Such low light levels are particularly prevalent in the polar regions. Keeping this simple analysis in mind, we now proceed with accurate calculations.

As stated in the introduction, ozone depletion will not only increase the amount of harmful UVB radiation, but also the amount of beneficial visible radiation (PUR). This follows from the spectral absorption cross section of ozone (Fig. 2A). Note that Fig. 2B and Fig. 2C show that at large solar zenith angles (i.e., when the sun is close to the horizon), the ratio of increased visible radiation to increased UVR is larger than for small solar zenith angles. Besides ozone absorption, this is also caused by molecular (Rayleigh) scattering and, to some extent, by aerosol scattering, which selectively scatter more UVR than PUR out of the atmosphere. At large solar zenith angles, the solar beam has to penetrate a larger optical depth; thus, a larger fraction of light with shorter wavelengths will be scattered out of and absorbed by the atmosphere. In the extreme case, if all UVR were removed by scattering, an ozone depletion would increase the magnitude of PUR but would not increase the magnitude of UVR.

At low solar elevations, the photosynthesis is largest in the surface water. But as the sun gets higher in the sky, UVR inhibits photosynthesis in the surface water, giving a maximum value for photosynthesis at a certain depth (Fig. 3). We see that even though UVR inhibits the production strongly in the upper part of the column, the difference in production from a 50% depletion in ozone is very small (barely visible in Fig. 3).

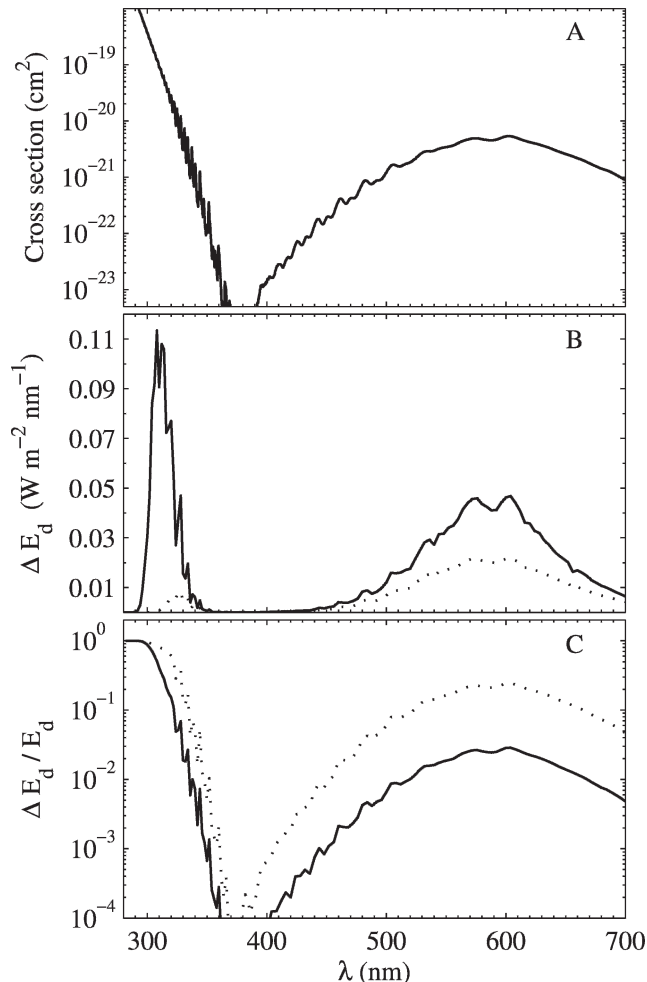


Fig. 2. (A) Absorption cross section of ozone at 261 K (Voigt et al. 2001). (B) Computed difference in downward surface irradiance caused by a reduction in the ozone column from 400 to 200 DU. The dotted and solid lines correspond to large and small solar zenith angles (SZA; i.e., $\mu_0 = 0.1$ [SZA = 84°] and $\mu_0 = 1.0$ [SZA = 0°]), respectively. (C) Same as panel B, except that now ΔE_d is computed relative to the downward surface irradiance E_d .

Note that for high levels of PUR production reaches saturation (Eq. 1). Thus, at small solar zenith angles, the small reduction in photosynthesis caused by ozone depletion cannot be explained by increased PUR tending to counteract UVR inhibition. This behavior points to another important issue concerning photosynthesis and ozone depletion. When weighted by the action spectrum for UVR-induced inhibition of photosynthesis, only UVR at wavelengths shorter than about 340 nm is significantly affected by the ozone layer (see Fig. 4). Therefore, the integral in Eq. 3, which extends from 280 to 400 nm, does not increase significantly when the ozone layer is depleted. Figure 4 shows that the increase of E^* is only 17% for a 50% ozone reduction, which gives a reduction of $1/(1 + E^*)$ of only 0.7%.

From Fig. 5 we see that a 50% reduction in the total ozone column results in a reduced level of photosynthesis only in that part of the water column that is above a certain depth. Below this depth, which decreases with solar

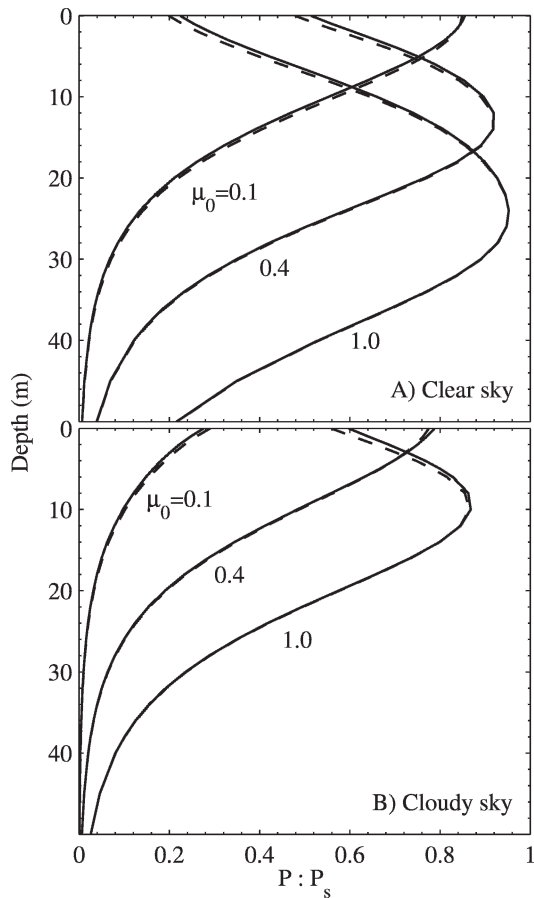


Fig. 3. Computed normalized photosynthesis $P:P_s$ (Eq. 1) in open water for varying solar zenith angles (i.e., for $\mu_0 = 0.1$ [SZA = 84°], $\mu_0 = 0.4$ [SZA = 66°], and $\mu_0 = 1.0$ [SZA = 0°]). Solid and dashed lines correspond to ozone concentrations of 400 and 200 DU, respectively. Input from Table 1 was used in the computations.

elevation, photosynthesis increases. At sufficiently low solar elevations, photosynthesis increases at all depths. At a fixed depth, the change from reduced to increased photosynthesis might be explained by considering Eq. 4. When the UVR level approaches zero, so does $E^*/(1 + E^*)$, whereas $E'/(e^{E'} - 1)$ always remains larger than zero (except for very high values of PUR). Thus, dP/P is positive if dE'/E' is positive, which means that at sufficiently low UVR values, photosynthesis will always increase, caused by increased PUR under ozone depletions. The UVR levels decrease with depth in the water. In polar waters, the typical depths at which the UVR levels at 305, 320, 340, and 380 nm are attenuated to 1% of their surface values are in the range of 5–10, 10–20, 15–30, and 20–70 m, respectively (Erga et al. 2005). At a certain critical depth, the PUR level becomes so low that dP/P changes from negative to positive values, and for a sufficiently low solar elevation, the PUR level becomes low enough to cause increased photosynthesis at the surface. It might be questionable to consider a Chl *a* concentration that remains constant with depth in polar regions because the growth season normally starts in the surface water of the marginal ice zone. However, later in the

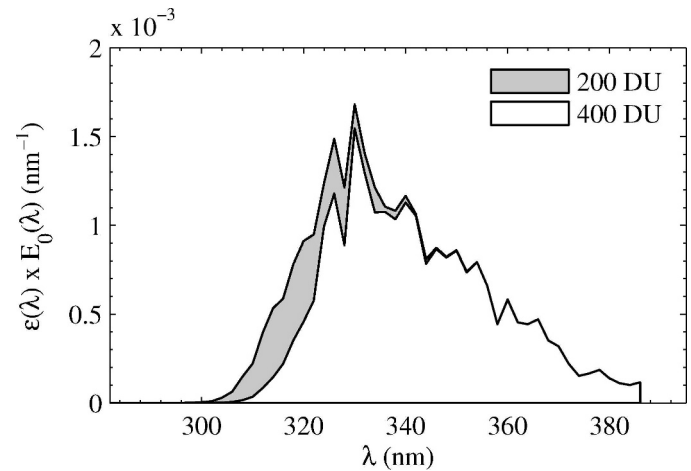


Fig. 4. Computed UVR action spectrum $\epsilon(\lambda)$ times surface spectral irradiance $E_0(\lambda)$ for total ozone column amounts of 200 and 400 DU under clear sky conditions for $\mu_0 = 0.2$ (SZA = 78°). The area under each of the curves gives the value of Eq. 3 and equals 0.054 and 0.046 for 200 and 400 DU, respectively.

year, the phytoplankton descends deeper into the water column as the ice edge recedes. Thus, in nutrient impoverished and well-mixed central waters, the phytoplankton biomass often is uniformly distributed down to about 20 m, with typical Chl *a* concentrations ranging from 0.1 to 2 mg m^{-3} . Also, blooms of phytoplankton appear to be rather common in unstratified waters, resulting in a relatively uniform distribution of biomass (Eilertsen and Taasen 1984).

It is clear that increased UVB radiation caused by ozone depletion only leads to a small decrease in photosynthesis in the upper part of the open water, particularly at high solar elevations. But increased PUR caused by ozone depletion

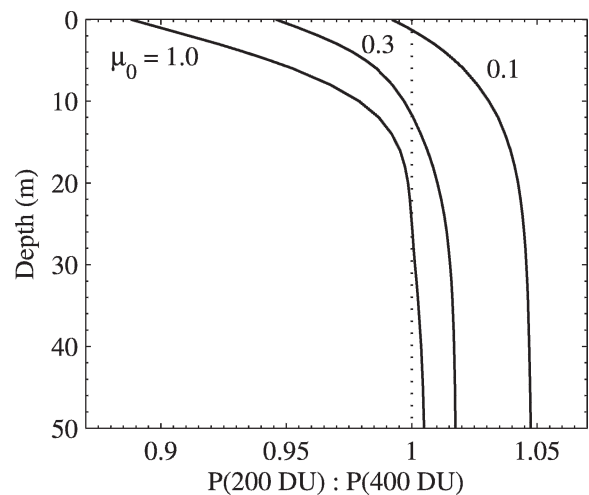


Fig. 5. Computed change in open water primary production caused by a 50% ozone depletion versus depth in the open water for $\mu_0 = 1.0$ (SZA = 0°), $\mu_0 = 0.3$ (SZA = 74°), and $\mu_0 = 0.1$ (SZA = 84°). $P(200\text{ DU}) : P(400\text{ DU})$ is the ratio of production in total ozone columns of 200 and 400 DU. Note the high resolution on the horizontal axis. Input from Table 1 was used in the computations.

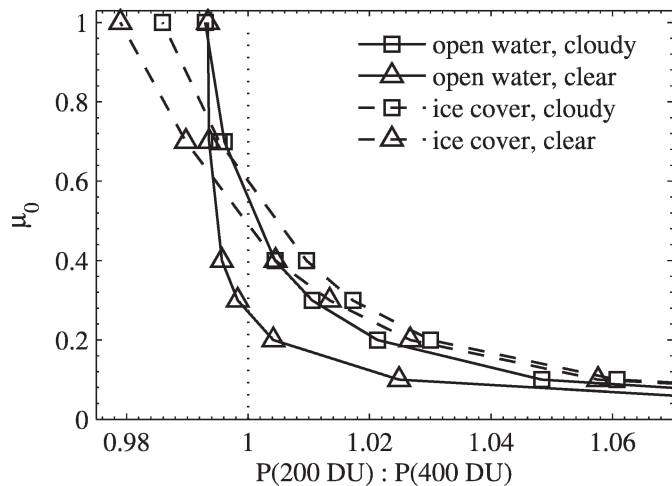


Fig. 6. Computed depth-integrated primary production ratio $P(200 \text{ DU}) : P(400 \text{ DU})$ for both open and ice-covered water caused by a 50% ozone depletion versus the cosine μ_0 of the solar zenith angle. Input from Table 1 was used in the computations, and the cut-off depth for the integration was 100 m.

leads to *increased* photosynthesis, particularly at low solar elevations, but also below a certain critical depth for high solar elevations in open water (Fig. 5) and at the bottom of snow-covered sea ice (Fig. 6). The question is: Which of these two effects will dominate? From Fig. 6, we see that the answer to this question is determined by the average solar zenith angle. If the average solar zenith angle is larger than a certain value, photosynthesis will be enhanced. To obtain the monthly averaged photosynthesis ratio during spring and summer, we integrated Eq. 1 over each month with ozone concentrations of 200 and 400 DU, and then we formed the ratio between these two integrated productivities. Figure 7 shows a pronounced high value of this ratio early in the spring and a smaller value in the late spring and summer. For this latitude (70°N , with input from Table 1), we found an increased average photosynthesis for all months. Note that the same results will be valid for Antarctica half a year later (ignoring the effect of the difference in sun–earth distance). Comparing Fig. 6 with the yearly average of the solar elevation shown in Fig. 8, we see that, at least for latitudes between the polar circle and the pole, the average solar zenith angle seems to be large enough to give an average net increase in primary production.

Figure 9 shows detailed computations of yearly averages of production ratios, wherein we have integrated photosynthesis in Eq. 1 in the same way as in Fig. 7, but now for a full year instead of month by month. We see that the computation with input from Table 1 gives a small increase in the primary production for latitudes above 50 degrees for both open water (oceanic) algae and for algae growing in the ice. The sensitivity analysis shown in Fig. 9 indicates that only ice algal communities growing in bare sea ice or in sea ice covered with a very thin layer of snow may experience a reduction in photosynthesis. This reduction occurs because the ice algae stay fixed close to the surface, covered only with a relatively transparent layer of snow

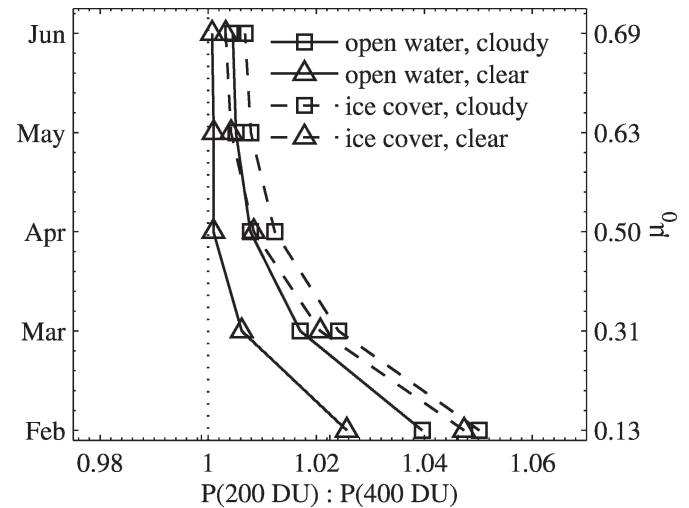


Fig. 7. Monthly averaged photosynthesis ratio $P(200 \text{ DU}) : P(400 \text{ DU})$ for open and ice-covered water caused by a 50% ozone depletion at 70°N . The axis to the right gives cosine of the solar zenith angle at midday midmonth. Input from Table 1 is used in the computations.

and ice. If impurities had been included in the snow and ice, the values for the ratio of $P(200 \text{ DU})$ to $P(400 \text{ DU})$ in Fig. 9 would have been higher. From the three panels, a rough estimate of the average increase in yearly averaged photosynthesis (or primary production) in the polar regions is found to be about 1%.

One should have in mind when taking the yearly average that the concentration of stratospheric ozone varies throughout the year, with ozone depletion episodes occurring most frequently in the spring. However, during spring, the average solar zenith angle is larger than the yearly average. The effect of this can be seen from the monthly averaged production at 70°N (Fig. 7), which shows that during the spring, primary production can

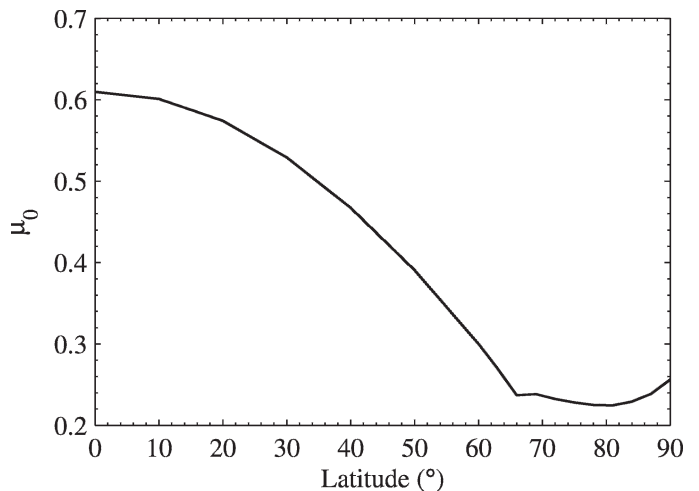


Fig. 8. Yearly time average of the cosine of the solar zenith angle, including only time periods when the sun is above the horizon. The calculations are done with the use of `sun_position.m` from www.mathworks.com. The kink in the graph at the polar circle results from excluding all-day winter darkness.

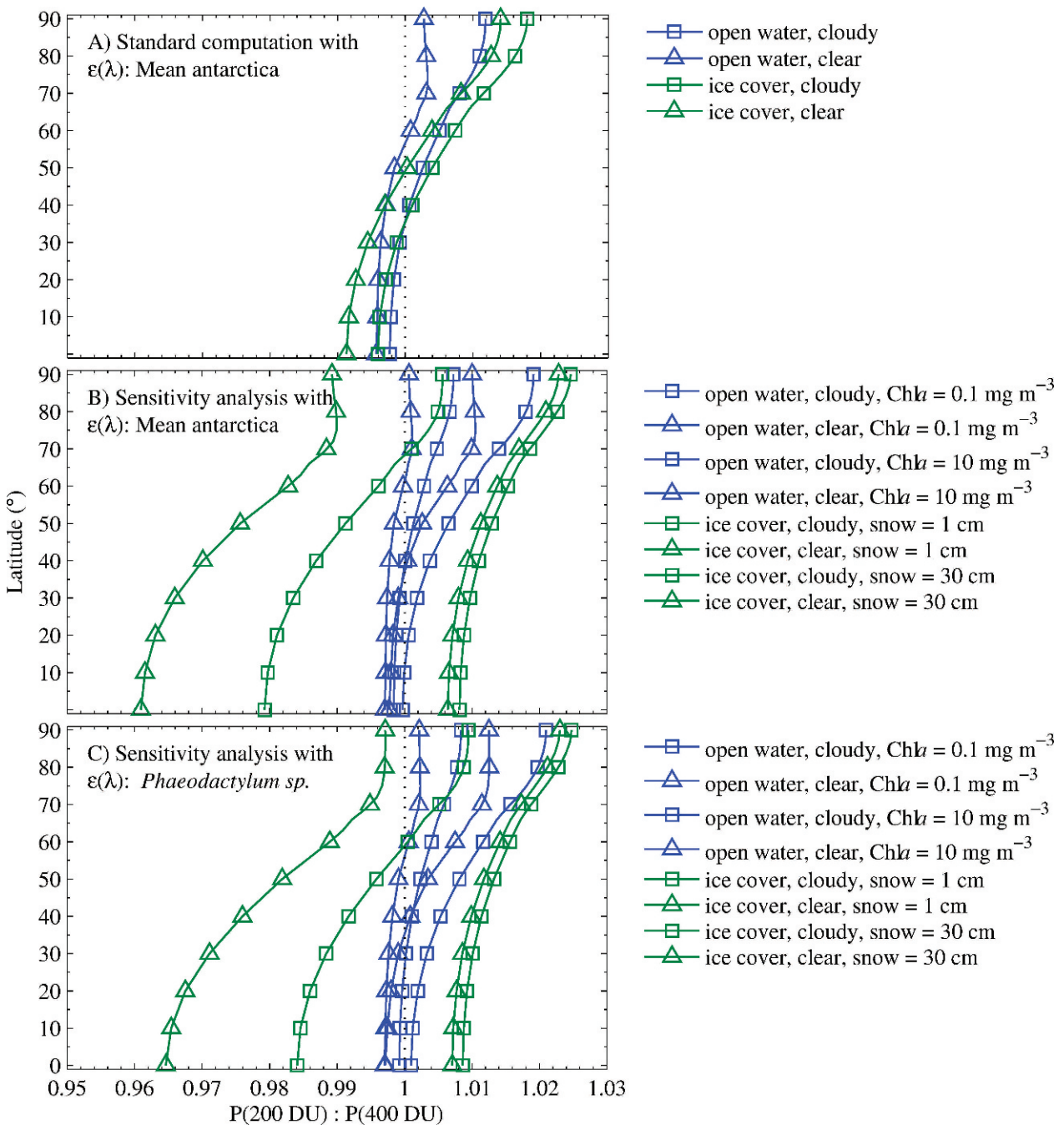


Fig. 9. Computed yearly averages of the depth-integrated primary production ratios $P(200 \text{ DU}) : P(400 \text{ DU})$ for open and ice-covered water caused by a 50% ozone depletion. (A) Computation with inputs from Table 1. (B) Computations with varying snow thickness and $Chl a$ concentration. (C) Same as panel B, but with an action spectrum $\epsilon(\lambda)$ for *Phaeodactylum* sp. (Cullen et al. 1992).

increase by between 0.1% and 5%. On average, this increase is larger than the estimated yearly averaged increase, which ranges from 0.5% to 1.4% at this latitude (Fig. 9A). Thus, spring values for increased primary production in polar regions could be even larger than the yearly estimate of about 1%.

As far as we know, our results are the first to indicate a possible enhanced yearly averaged primary production resulting from ozone depletion. Note, however, that Arrigo et al. (2003) found the loss in total spring primary

production caused by ozone depletion to be $<0.25\%$, which is close to no loss. Also, note that small changes in primary production caused by ozone depletion make it difficult to quantify such changes by in situ measurements. It is very hard to distinguish effects caused by ozone depletion from those caused by variations in cloudiness, aerosol concentration, water turbidity, and so on. Even for phytoplankton samples placed in vessels with protective coatings, which give varying degrees of UVR exposure, it is difficult to quantify the change because this method does

not normally account for increased PUR when comparing two vessels with different degrees of UVR coating. Fortunately, with a model, it is possible to keep all other variables, except the ozone concentration, constant. Hence, by combining well-tested biological and optical parameterizations, we can analyze small variations in the primary production caused by variations in the ozone layer. For completeness we should mention that our model does not account for other possible effects of increased UVR, such as shifts in species composition, diminished grazing, and changes in the nutrient balance.

On the basis of our calculations using a comprehensive radiative transfer model in combination with a parameterization of oceanic primary production, we conclude that (1) ozone depletion not only increases harmful UVR, but also increases beneficial visible radiation; (2) the beneficial effects of increased visible radiation dominates over the deleterious effects of increased UVR in protected environments (i.e., for phytoplankton growing under sea ice and below a certain depth in open waters at high latitudes with low solar elevations); and (3) a large fraction of the primary production in the polar regions is caused by ice algae, which grow in environments that are very well protected from UVR. From these considerations and from our calculations, we estimate that primary production in the polar regions could increase by approximately 1% under a 50% ozone depletion. Our estimate is conservative because we have ignored the effect of impurities in snow and ice and enhanced levels of colored dissolved organic matter (CDOM) in the water. Such impurities and CDOM absorb relatively more in the UV than the the visible part of the spectrum and could therefore lead to a small enhancement of our estimated 1% increase in primary production because of ozone depletion. Because our assessment contradicts previous studies, which show diverging results, we hope that in the future, collaborative efforts in this important interdisciplinary field may add new insights into the effects of ozone depletion on aquatic ecosystems.

References

- ANDERSEN, G. P., S. A. CLOUGH, F. X. KNEIZYS, J. H. CHETWYND, AND E. P. SHETTLE. 1986. AFGL atmospheric constituent profiles (0–120 km). AFGL-TR-86-0110, AFGL (OPI), Hanscom AFB, MA.
- ARRIGO, K. R. 1994. Impact of ozone depletion on phytoplankton growth in the Southern Ocean: Large-scale spatial and temporal variability. *Mar. Ecol. Prog. Ser.* **114**: 1–12.
- , D. LUBIN, G. L. VAN DIJKEN, O. HOLM-HANSEN, AND E. MORROW. 2003. Impact of a deep ozone hole on Southern Ocean primary production. *J. Geophys. Res.* **108**: C53154, doi:10.1029/2001JC001226.
- AUSTIN, J., N. BUTCHART, AND K. P. SHINE. 1992. Possibility of an Arctic ozone hole in a doubled-CO₂ climate. *Nature* **360**: 221–225.
- CULLEN, J. J., P. J. NEALE, AND M. P. LESSER. 1992. Biological weighting function for the inhibition of phytoplankton photosynthesis by ultraviolet radiation. *Science* **258**: 646–650.
- EILERTSEN, H. C., AND J. P. TAASEN. 1984. Investigations on the plankton community of Balsfjorden, northern Norway. The phytoplankton 1976–1978. Environmental factors, dynamics of growth, and primary production. *Sarsia* **69**: 1–15.
- ERGA, S. R., AND OTHERS. 2005. UV transmission in Norwegian marine waters: Controlling factors, and possible effects on primary production and vertical distribution of phytoplankton. *Mar. Ecol. Prog. Ser.* **305**: 79–100.
- GJERSTAD, K. I., J. J. STAMNES, B. HAMRE, J. K. LOTSBERG, B. YAN, AND K. STAMNES. 2003. Monte Carlo and discrete-ordinate simulations of irradiances in the coupled atmosphere–ocean system. *Appl. Opt.* **42**: 2609–2622.
- HÄDER, D. P. [ED.]. 1997. The effects of ozone depletion on aquatic ecosystems. Academic.
- HAMRE, B., J.-G. WINTHER, S. GERLAND, J. J. STAMNES, AND K. STAMNES. 2004. Modeled and measured transmittance of snow covered first year sea ice in Kongsfjorden, Svalbard. *J. Geophys. Res.* **109**: C1006, doi:10.1029/2003JC001926.
- HOLM-HANSEN, O., E. W. HELBLING, AND D. LUBIN. 1993. Ultraviolet radiation in Antarctica: Inhibition of primary production. *Photochem. Photobiol.* **58**: 567–570.
- JIN, Z., AND K. STAMNES. 1994. Radiative transfer in nonuniformly refracting layered media: Atmosphere–ocean system. *Appl. Opt.* **33**: 431–442.
- , K. STAMNES, W. F. WEEKS, AND S. C. TSAY. 1994. The effect of sea ice on the solar energy budget in the atmosphere–sea ice–ocean system: A model study. *J. Geophys. Res.* **99**: 25,281–25,294.
- JOHNSEN, G., AND E. N. HEGSETH. 1991. Photoadaptation of sea-ice microalgae in the Barents Sea. *Polar Biol.* **11**: 179–184.
- MOREL, A. 1974. Optical properties of pure seawater, p. 1–24. *In* N. G. Jerlov and E. S. Nelson [eds.], *Optical aspects of oceanography*. Academic.
- NEALE, P. J., J. J. CULLEN, AND R. F. DAVIS. 1998a. Inhibition of marine photosynthesis by ultraviolet radiation: Variable-sensitivity of phytoplankton in the Weddell–Scotia Confluence during the austral spring. *Limnol. Oceanogr.* **43**: 433–448.
- , R. F. DAVIS, AND J. J. CULLEN. 1998b. Interactive effects of ozone depletion and vertical mixing on photosynthesis of Antarctic phytoplankton. *Nature* **392**: 585–588.
- PRIEUR, L., AND S. SATHYENDRANATH. 1981. An optical classification of coastal and oceanic waters based on the specific spectral absorption of phytoplankton pigments, dissolved organic matter and particulate materials. *Limnol. Oceanogr.* **26**: 671–689.
- SAKSHAUG, E., G. JOHNSEN, K. ANDRESEN, AND M. VERNET. 1990. Modeling of light-dependent algal photosynthesis and growth: Experiments with the Barents Sea diatoms *Thalassiosira nordenskiöldii* and *Chaetoceros furcellatus*. *Deep-Sea Res.* **38**: 415–430.
- SHETTLE, E. P., AND R. W. FENN. 1976. Models of atmospheric aerosols and their optical properties. *In* AGARD Conference proceedings 183, *Optical propagation in the atmosphere*.
- SMITH, R. C., ———. 1992. Ozone depletion: Ultraviolet radiation and phytoplankton biology in Antarctic waters. *Science* **255**: 952–957.
- STAEHELIN, J., N. R. P. HARRIS, C. APPENZELLER, AND J. EBERHARD. 2001. Ozone trends: A review. *Rev. Geophys.* **29**: 231–290.
- THOMAS, G. E., AND K. STAMNES. 1999. *Radiative Transfer in the Atmosphere and Ocean*. Cambridge Univ. Press.
- VOIGT, S., J. ORPHAL, K. BOGUMIL, AND J. P. BURROWS. 2001. The temperature dependence (203–293 K) of the absorption cross section of O₃ in the 230–850 nm region measured by Fourier-transform spectroscopy. *J. Photochem. Photobiol. A* **143**: 1–9.

Received: 31 October 2006

Accepted: 21 June 2007

Amended: 27 August 2007